Psychoradiology, 2023, **3**, 1–10
DOI: 10.1093/psyrad/kkad012
Advance access publication date: 21 July 2023
Research Article

Neural substrates of behavioral inhibitory control during the two-choice oddball task: functional neuroimaging evidence

Shirui Zhao[1,2,#], Ruosong Yuan[3,#], Wei Gao[1], Qiang Liu[1] and Jiajin Yuan[1,4,*]

[1]The Affect Cognition and Regulation Laboratory (ACRLab), Institute of Brain and Psychological Sciences, Sichuan Normal University, Chengdu 610066, China
[2]Faculté des Sciences Psychologiques et de l'Éducation, Université Libre de Bruxelles (ULB) Brussels 1050, Belgium
[3]Faculty of Psychology, Southwest University, Chongqing 400715, China
[4]Sichuan Key Laboratory of Psychology and Behavior of Discipline Inspection and Supervision (Sichuan Normal University), Chengdu 610066, China
*Correspondence: Jiajin Yuan, yuanjiajin168@126.com
#Zhao S. and Yuan R. contributed equally to this work

Abstract

Background: Behavioral inhibitory control (BIC) depicts a cognitive function of inhibiting inappropriate dominant responses to meet the context requirement. Despite abundant research into neural substrates of BIC during the go/no-go and stop signal tasks, these tasks were consistently shown hard to isolate neural processes of response inhibition, which is of primary interest, from those of response generation. Therefore, it is necessary to explore neural substrates of BIC using the two-choice oddball (TCO) task, whose design of dual responses is thought to produce an inhibition effect free of the confounds of response generation.

Objective: The current study aims at depicting neural substrates of performing behavioral inhibitory control in the two-choice oddball task, which designs dual responses to balance response generation. Also, neural substrates of performing BIC during this task are compared with those in the go/no-go task, which designs a motor response in a single condition.

Methods: The present study integrated go/no-go (GNG) and TCO tasks into a new Three-Choice BIC paradigm, which consists of standard (75%), deviant (12.5%), and no-go (12.5%) conditions simultaneously. Forty-eight college students participated in this experiment, which required them to respond to standard (frequent) and deviant stimuli by pressing different keys, while inhibiting motor response to no-go stimuli. Conjunction analysis and ROI (region of interest) analysis were adopted to identify the unique neural mechanisms that subserve the processes of BIC.

Results: Both tasks are effective in assessing BIC function, reflected by the significantly lower accuracy of no-go compared to standard condition in GNG, and the significantly lower accuracy and longer reaction time of deviant compared to standard condition in TCO. However, there were no significant differences between deviant and no-go conditions in accuracy. Moreover, functional neuroimaging has demonstrated that the anterior cingulate cortex (ACC) activation was observed for no-go vs. standard contrast in the GNG task, but not in deviant vs. standard contrast in the TCO task, suggesting that ACC involvement is not a necessary component of BIC. Second, ROI analysis of areas that were co-activated in TCO and GNG showed co-activations in the right inferior frontal cortex (triangle and orbital), with the signals in the TCO task significantly higher than those in the GNG task.

Conclusions: These findings show that the designed responses to both standard and deviant stimuli in the TCO task, compared to the GNG task, produced a more prominent prefrontal inhibitory processing and extinguished an unnecessary component of ACC activation during BIC. This implies that prefrontal involvement, but not that of ACC, is mandatory for the successful performance of inhibiting prepotent behaviors.

Keywords: behavioral inhibitory control; two-choice oddball; go/no-go; fMRI

Introduction

Behavioral inhibitory control (BIC) refers to a cognitive function of refraining from inappropriate and impulsive behaviors to meet environmental requests (Criaud & Boulinguez, 2013; Yuan *et al.*, 2017, 2020). The BIC function plays an important role in humans' adaptiveness to environmental changes, and BIC dysfunction has been implicated in several mental and behavioral disorders, such as aggression (Smits *et al.*, 2004), substance abuse (Bickel *et al.*, 2011; Houben *et al.*, 2011), attention-deficit hyperactivity disorder (Alderson *et al.*, 2017), and schizophrenia (Bellgrove *et al.*, 2006; Cooper & Hughes, 2018). Therefore, effective assessment of individual variations of BIC, as well as understanding the neural markers of BIC, is important for the diagnosis and treatment of BIC-related disorders.

For decades, the go/no-go (GNG) task and stop signal task (SST) have been accepted as effective measures of humans' BIC function (Garavan *et al.*, 2003; Simmonds *et al.*, 2008; Ren *et al.*, 2019; Qiu, & Wang, 2021; Wolpe *et al.*, 2022; Wilbertz *et al.*, 2014). Regularly, the GNG task has been associated with the presentation of two stimulus cues with different onset frequencies. The onset of one frequent stimulus (such as W) required participants to perform a motor response (like button-press) while the presentation of the other infrequent one (e.g. M) required participants to withhold a response. The contrast of no-go and go conditions in

Received: 25 May 2023; **Revised:** 21 June 2023; **Accepted:** 20 July 2023

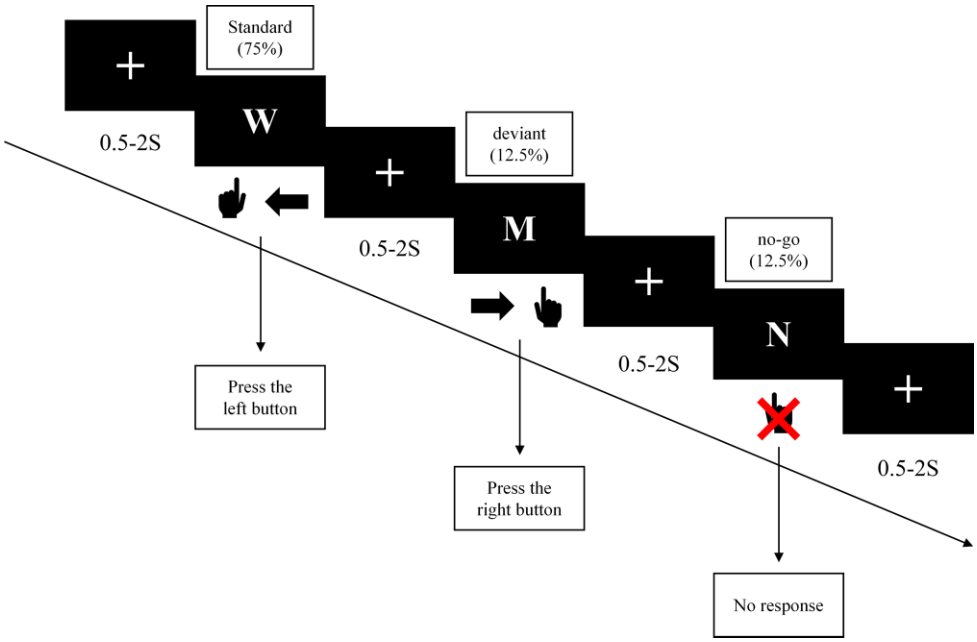

Figure 1: The Three-Choice BIC paradigm that combined the TCO and GNG task. Participants were asked to press button 2 when they saw the standard stimulus "W," and press button 3 when they saw the deviant stimulus "M." No response should be made when seeing the no-go stimulus "N."

behavioral accuracy and neuroimaging data was thought to reflect individual differences in BIC (Goldstein *et al.*, 2007; Yu *et al.*, 2009; Dong *et al.*, 2010). With regard to SST, individuals' indication of BIC comes from the "stop signal," which is embedded in a sequence of go trials. The stop-signal reaction time (SSRT), which reflects the average time required to successfully cancel a planned movement in ~50% of stop trials, is used to assess one's inhibitory control performance (Logan & Cowan, 1984; Mancini *et al.*, 2022). A shorter SSRT indicates a quicker time for a person to cancel the action, thus denoting a better performance of inhibitory control.

Based on GNG task and SST, numerous studies have investigated neural substrates of BIC using functional neuroimaging techniques. For instance, functional magnetic resonance imaging (fMRI) studies have indicated that the inferior frontal gyrus (IFG), pre-supplementary motor area (pre-SMA), and anterior cingulate cortex (ACC) are involved in BIC (Hester *et al.*, 2004; Goldstein *et al.*, 2007; Aron *et al.*, 2014; Wrege *et al.*, 2014; Qiu & Wang, 2021). In more detail, the function of these regions has also been widely addressed. It has been indicated that the IFG activity increases significantly when individuals need to work harder at inhibitory control (Suarez-Suarez *et al.*, 2020). Some studies highlighted the role of right IFG in BIC, in that the rIFG implements inhibition via the connections to the prefrontal-basal ganglia network (Aron *et al.*, 2004; Aron *et al.*, 2014). However, some studies using the SST observed bilateral activations in the IFG (Cai and Leung, 2009; Li *et al.*, 2006). Some studies using SST task indicated that the pre-SMA is a critical region for inhibition (Chao *et al.*, 2009; Lee *et al.*, 2016; Wang *et al.*, 2019). Duann and colleagues (2009) found that response inhibition will not occur until the stop signal reaches the pre-SMA, and the role of IFG in BIC lies in its correlation with attention processing. However, the pre-SMA activation in the GNG task reflects response conflict monitoring and is thus sensitive to conflict manipulation (Hester *et al.*, 2004; Garavan *et al.*, 2003). Moreover, ACC is another activation foci underpinning behavioral inhibitory processing, as reported in previous studies (Carter *et al.*, 1998). Ma and colleagues (2015) demonstrated that cocaine-dependent patients perform inhibitory control through the monitoring function of the ACC rather than that of frontal cortex (Ma *et al.*, 2015). Despite being also active during error detection (Orr & Hester, 2012), ACC has long been considered to reflect conflict monitoring instead of error detection (Carter *et al.*, 1998). All the evidence obtained from GNG or stop-signal tasks suggests that IFG, ACC, and pre-SMA are important neural substrates of humans' BIC function.

However, on the one hand, behavioral index of BIC during the GNG task relies solely on error rates, and this index was indicated to be less sensitive, often statistically insignificant between go and no-go conditions (Todd *et al.*, 2008; Bokura *et al.*, 2001), or less capable of discriminating individual differences that was existent inherently (Ren *et al.*, 2019); On the other hand, the design of single response in this task resulted in an obscuring effect in which the effect of response inhibition in no-go trials cannot be isolated from that of response generation in Go trials (Yuan *et al.*, 2012). For example, using an event-related potential technique, Smith *et al.* (2008) have indicated the electrophysiological markers of BIC were contaminated by movement-related positive potentials overlapping with the time windows of no-go-P3. Although the SST generated SSRT as an indicator of BIC, this indicator is not a direct measure, but is computed by subtracting the critical 50% stop-signal delay latency from the mean primary go task reaction time (RT); the acquisition of the critical stop-signal delay was again influenced by the choice of initial stop-signal delay and varying interval (Wöstmann *et al.*, 2013; Yuan *et al.*, 2017). Also, the N2/P3 evoked by the stop signal overlaps with the stimulus-induced event-related potential component, producing confounds of neural signals (Kok *et al.*, 2004).

Nevertheless, these limitations can be overcome by using a two-choice oddball (TCO) task, where two distinct button-press responses were designed in response to the frequent and infrequent stimuli, respectively. By counterbalancing stimulus-response contingencies across participants, this paradigm has been evidenced to be sensitive in detecting BIC-related individual differences, such as emotional modulation (Yuan *et al.*, 2012), addictive impact (Zhao *et al.*, 2015; Yuan *et al.*, 2020), or cognitive training effect (Ren *et al.*, 2019), in the absence of the

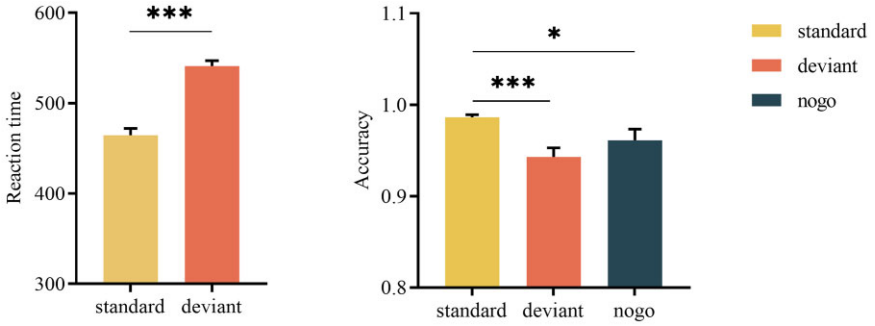

Figure 2: The averaged RT (left) and accuracy (right) as well as multiple comparisons during standard, deviant and no-go trials (error bars denote SEM, $^{*}P < 0.05$; $^{***}P < 0.001$)

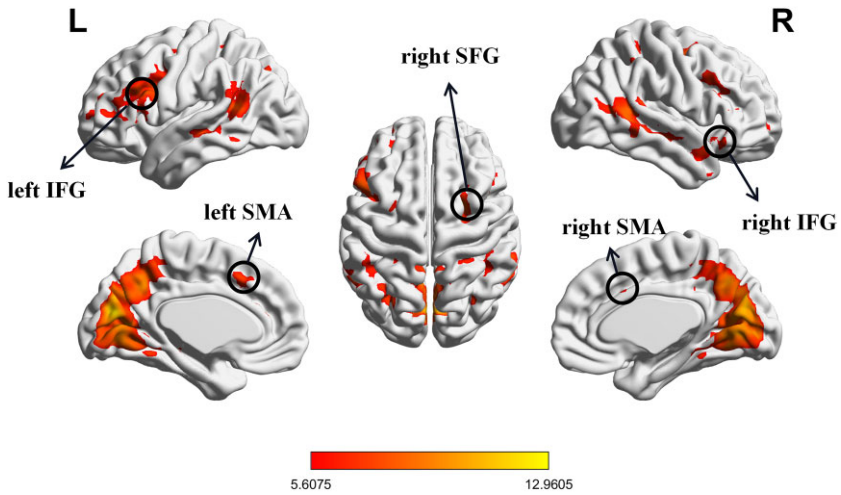

Figure 3: Results of the direct comparison between standard and no-go conditions (no-go > standard). Data are thresholded at FWE $P < 0.01$, with a cluster-level of $k > 20$.

above-mentioned confounds as reported in the GNG or SST tasks. Although neural substates of BIC have been widely addressed (Aron *et al.*, 2014; Chiu & Egner, 2015; Schel *et al.*, 2014; Wrege *et al.*, 2014; Wang *et al.*, 2019; Ma *et al.*, 2015), the BIC-specific neural underpinnings should be revisited and clarified after controlling the previously mentioned limitations, for example, using the TCO task.

Therefore, in the current study, we integrated the classic GNG with the TCO paradigm, to design an updated version of TCO task allowing comparisons between the two paradigms within a single task. We chose to compare go/nogo and TCO task, mainly because the two paradigms share a similarity in stimulus onset frequency, and in the pattern of stimulus discrimination and response selection, except that the former required response withholding while the latter required an alternative response. By contrast, the stop-signal task differs in many dimensions from the TCO task, including the insertion of stop signal following go stimulus, and the variations of stop-signal delay and so on. These lead to more difficulties in directly comparing stop-signal with TCO tasks.

The updated task, which combines go/nogo and TCO paradigms in the current study, consists of three stimuli: a frequent standard stimulus requiring one button-press, an infrequent deviant stimulus requiring the other button-press, and an infrequent no-go stimulus whose presentation requires withholding of motor response. Deviant and no-go stimuli were presented with equal frequency. Consequently, deviant-standard contrast in outcome variables represents the assessment of BIC in the TCO task while no-go-standard contrast represents that in the GNG task. Moreover, the direct comparison between these two contrasts shows the differences from the GNG to the TCO task in neural substrates of behavioral inhibitory processing. Specifically, given that both tasks have proved effective in assessing BIC, we hypothesize both may activate the key regions implicated in BIC, such as IFG, precuneus, and ACC. However, in regions involving motor processing, such as SMA and pre-SMA, the TCO task should show less activity compared to the GNG task as a result of balanced responses to both standard and deviant stimuli.

Methods

Participants

Forty-eight college students participated in this experiment. One participant with excessive head movement (excluding criteria 3.0 mm and 3.0° in maximum head motion) and another with low accuracy were removed from further analysis. Thus, the data from 46 participants (21 males, 25 females, average age 21.3 ± 2.62 years) were included in the formal analysis. All the participants were right-handed, had normal or corrected-to-normal vision, and had no attention deficit or learning disabilities. This study was approved by the ethical committee of the local university. All the participants gave written informed consent and were paid for their participation.

Table 1: Brain regions activated by no-go > standard contrast (GNG).

	Region (AAL)	Hemispheres	Peak MNI coordinates			t	Voxel
			x	y	z		
Cluster1	Temporal _ Mid	L	−51	−6	−18	6.69	31
	Temporal _ Inf	L					
Cluster2	Frontal_ Inf _ Orb	R	42	21	−15	7.13	208
	Temporal _ Pole_ Sup	R					
	Insula	R					
	Temporal Pole _ Mid	R					
	Temporal _ Mid	R					
Cluster3	Precuneus	L/R	−3	−78	18	12.96	4627
	Calcarine	L/R					
	Lingual	L/R					
	Parietal _ Inf	L/R					
	Cuneus	L/R					
	SupraMaginal	L/R					
	Occipital _ Mid	L					
	Fusiform	L/R					
	Occipital _ Sup	L/R					
	Cingulum _ Mid	L/R					
	Temporal _ Mid	L					
	Angular	L					
	Parietal _ Inf	L/R					
	Postcental	L					
	Temporal _ Sup	L					
	ParaHippocampal	L					
Cluster4	Temporal _ Mid	R	60	−48	6	9.10	892
	Temporal _ Sup	R					
	Angular	R					
	Occipital _ Mid	R					
	SupraMaginal	R					
	Occipital _ Sup	R					
Cluster5	Temporal _ Mid	L	−57	−24	−9	8.20	327
	Temporal _ Inf	L					
	Temporal _ Sup	L					
Cluster6	Frontal _ Inf _ Tri	L	−51	18	27	8.46	949
	Frontal _ Mid	L					
	Frontal _ Inf _ Oper	L					
	Pretcental	L					
	Frontal _ Sup	L					
Cluster7	Frontal _ Inf _ Tri	R	42	36	12	6.34	33
Cluster8	Frontal _ Mid	R	27	3	54	8.49	351
	Frontal _ Inf _ Tri	R					
	Frontal _ Sup	R					
	Frontal _ Inf _ Oper	R					
	Pretcental	R					
Cluster9	Cingulum _ Ant	L	−3	18	45	7.80	191
	Supp _ Motor _ Area	L					
	Frontal _ Sup _ Medial	L					
	Cingulum Mid	L/R					

AAL: anatomical automatic labeling; L: left; R: right. Data thresholded at FWE $P < 0.01$, with a cluster-level of $k > 20$

Procedure

First, participants were asked to sign the informed consent form and an MRI safety screening form, then they performed a practice session, and only when the accuracy rate of the practice reached 100% did the participants enter the formal experiment and start scanning. The formal experiment was the same as the practice (Fig. 1). The participants were required to press button 2 with their left index finger when they saw the standard stimulus (75% of total trials), and the right index finger to press button 3 when they saw the deviant stimulus (12.5% of total trials), and they did not press the button when they saw the no-go stimulus (12.5% of total trials). The stimulus presentation was terminated by the participant's button-press response or lasted for 1000 ms before the next trial began.

Functional MRI data acquisition

The experiment used a 3T superconducting MRI system (GE Discovery MR750) produced by Siemens, with an eight-channel head coil, and the head was fixed with a pad to prevent head movement. The gradient-echo planner imaging pulse sequence (GRE-EPI) was used for the functional images scanning and the relevant scanning parameters were: repetition time (TR) = 2000 ms, echo time (TE) = 30 ms, flip angle = 90°, thickness = 3.5 mm,

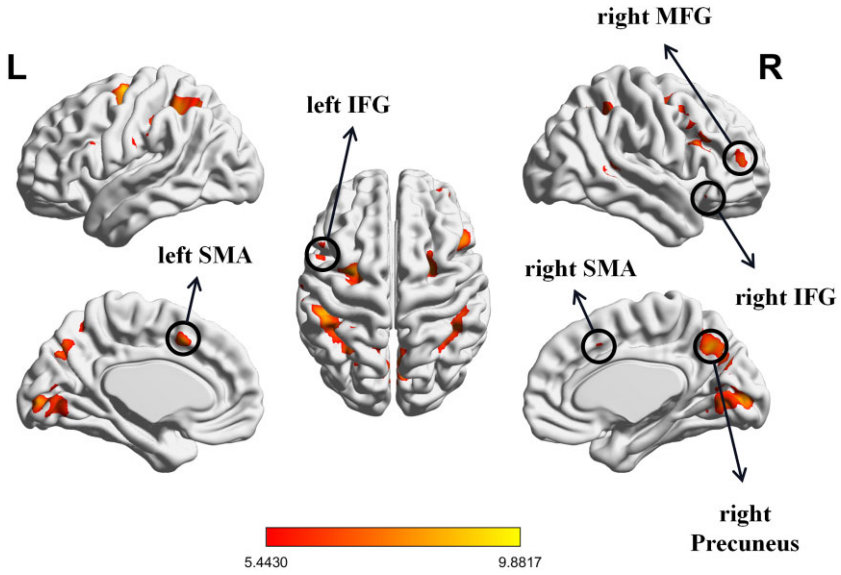

Figure 4: Results of the direct comparison between standard and deviant conditions (deviant > standard). Data are thresholded at FWE $P < 0.01$, with a cluster-level of $k > 20$.

slice gap = 0 mm, field of view (FOV) = 224 × 224 mm, scan matrix = 64 × 64, slice number = 33. A total of 221 whole-brain volumes were recorded. Stimulus presentation and behavioral data acquisition were obtained by E-prime software.

Preprocessing and Analysis

fMRI data were preprocessed stepwise by DPARSF (DPARSFA V5.2 http://rfmri.org/DPARSF) (Chao-Gan & Yu-Feng, 2010). First, we removed 10 time points to make sure the stable was signal. Then, the images were slice-time corrected, realigned to correct for participant motion, segmented by DARTEL, normalized to the Montreal Neurological Institute (MNI) space using the structure information from coregistration, and smoothed by DARTEL with a Gaussian kernel (9 mm full-width at half-maximum).

First-level analysis

The statistical analysis of the preprocessed functional data was performed with statistical parametric mapping (SPM12) tools (www.fil.ion.ucl.ac.uk) in MATLAB R2019a. Three conditions (standard, deviant, no-go) were adopted in the general linear model for the first-level analysis. Six realign parameters were further included as regressors for head motion effects, and they were convolved with a canonical hemodynamic response function.

Second-level analysis

Group analysis was also performed with SPM12 in MATLAB R2019a. To investigate the difference in the activation results between the GNG and the TCO, we compared each stimulus condition at the individual level (GNG results: no-go > standard; TCO results: deviant > standard). In the first level analysis, we obtained the whole-brain mean activations for each condition. We used the results of the first-level analysis as input to the second-level analysis and performed group-level analysis (paired t-test), using an family wise error (FWE) correction of $P < 0.01$ and a voxel threshold of $k > 20$ for multiple comparisons.

Conjunction analysis

The conjunction analysis allows the exploration of commonalities in the activation of participant groups performing different tasks in relation to functions that are common to the task (Rubia *et al.*, 2001): that is, a brain image analysis method similar to cognitive conjunction (Friston *et al.*, 1999). Mostofsky deemed that the research task of behavioral inhibition is related to the brain region activation of fMRI (Mostofsky & Simmonds, 2008), which means that the results we get from the paradigm cannot be independent of the task. Therefore, we use conjunction analysis to find the co-activated brain regions from different versions of behavioral inhibition tasks; these brain regions are likely to be the results of task-independent activation.

Results

Behavioral results

We calculated the participants' accuracy (ACC) for standard ($M = 0.99$, $SD = 0.02$), deviant ($M = 0.94$, $SD = 0.07$), and no-go stimulus ($M = 0.96$, $SD = 0.08$), and the RT to the standard ($M = 464.62$, $SD = 50.17$) and deviant stimulus ($M = 541.04$, $SD = 41.21$). A paired-sample t-test revealed that the RT is significantly shorter during standard compared to deviant trials ($t = -14.48$, $P < 0.001$). Repeated measures analysis of variance revealed a significant main effect of accuracy ($F = 8.617$, $P < 0.001$), and *post hoc* multiple comparison shows that the accuracy was significantly higher during standard than during deviant ($t = 4\,519$, $P < 0.001$) and no-go ($t = 2.051$, $P = 0.046$) trials; no significant accuracy differences were observed between deviant and no-go trials (Fig. 2)

fMRI results

Whole-brain activation of GNG task

In the contrast of no-go > standard, we used FWE ($P < 0.01$) for the correction of multiple comparisons, and set the cluster size to $k > 20$. We observed significant activation in the regions of superior, inferior, and middle frontal gyrus, precuneus, left SMA, fusiform, ACC, left frontal supplementary medial gyrus, precentral gyrus, and plenty of other regions (Fig. 3 and Table 1). Some

Table 2: Brain regions activated by the deviant > standard contrast (TCO).

	Region (AAL)	Hemispheres	Peak MNI coordinates			t	Voxel
			x	y	z		
Cluster1	Cerebelum_Crus1	L	−36	−66	−24	6.85	106
	Carcbelum_6	L					
	Fusiform	L					
Cluster2	Frontal_ Inf _ Orb	R	48	21	−12	8.43	51
	Temporal Pole_ Sup	R					
Cluster3	Parietal _ Inf	L	9	−66	39	9.74	1986
	Precuneus	R					
	Calcarine	L/R					
	Parietal _ Sup	L					
	Lingual	L/R					
	Postcental	L					
	Cuneus	L					
	SupraMaginal	L					
	Occipital _ Mid	L					
	Angular	L					
	Occipital _ Sup	L					
Cluster4	Parietal _ Inf	R	39	−42	36	8.00	471
	SupraMarginal	R					
	Temporal Mid	R					
	Angular	R					
	Temporal Sup	R					
	Postcentral	R					
Cluster5	Frontal _ Mid	R	36	51	12	7.41	103
	Frontal _ Sup	R					
Cluster6	Precentral	L	−51	9	33	6.95	73
	Frontal _ Inf _ Tri	L					
	Frontal _ Inf _ Oper	L					
Cluster7	Supp _ Motor _ Area	L/R	−3	12	42	8.00	125
	Cingulum _ Mid	L/R					
Cluster8	Precentral	L	−24	−9	63	9.88	235
	Frontal _ Sup	L					
	Frontal _ Mid	L					
	Supp_ Motor _ Area	L					
Cluster9	Frontal _ Mid	R		0	51	8.92	366
	Frontal _ Inf _ Tri	R					
	Frontal _ Inf _ Oper	R					
	Frontal _ Sup	R					
	Precentral	R					

AAL: anatomical automatic labeling; L: left; R: right. Data thresholded at FWE $P < 0.01$, with a cluster-level of $k > 20$

studies have suggested that the basal ganglia, such as the striatum, plays an important role in BIC (Korponay *et al.*, 2019; Jahanshahi *et al.*, 2015; Behan *et al.*, 2015a; Zavala *et al.*, 2014; Bjork *et al.*, 2012), but no relevant findings were found in the present study. We speculate that the basal ganglia did not survive due to the strict multiple comparison correction. In addition, we also find that insula and pre-SMA were activated, which were reported to be critical areas in BIC (Fig. 3).

Whole-brain activation of TCO task

In the contrast of deviant > standard, we use FWE ($P < 0.01$) for multiple comparisons correction, and set the cluster size to $k > 20$. We found significant activation in the regions of the left fusiform, superior, inferior, and middle frontal gyrus, precuneus, SMA, and other regions (Fig. 4 and Table 2). No significant activations were detected in the ACC and left frontal supplementary medial gyrus (pre-SMA).

Whole-brain activation of GNG vs. TCO task

We contrast the results of TCO with GNG. We found no survived voxels after FWE correction ($P < 0.01$) for multiple comparisons. Thus, the activation regions of the two paradigms are roughly the same, which leads to the lack of significant differences after contrast. Therefore, we further used conjunction analysis to explore the differences in the brain regions co-activated by the two paradigms.

Co-activation regions of GNG and TCO task

We saved the results of TCO and GNG after FWE multiple comparisons correction as masks, and later used the Image Calculate function in SPM12 to calculate the commonly activated brain regions of the two paradigms so as to get the paradigm-independent activated brain regions (Table 3). The results showed commonly activated regions in the right orbital IFG, precuneus, triangle IFG, right opercular IFG, middle frontal gyrus, superior frontal gyrus, left SMA, and other regions.

ROI analysis

We saved the regions that were co-activated in the GNG and TCO as the mask, and extracted signals of TCO and GNG in Response Exploration (REX www.neuroimaging.org.au/nig/REX/) (Duff *et al.*, 2007). Next, the values of the ROI in the two paradigms were

Table 3: Co-activation brain regions of GNG task and TCO task.

	Region (AAL)	Hemispheres	Voxel
Cluster1	Frontal_ Inf _ Orb	R	26
Cluster2	Temporal Mid	R	111
	Temporal _ Sup	R	
Cluster3	Precuneus	L/R	1158
	Calcarine	L	
	Lingual	L/R	
	Cuneus	L/R	
	Parietal _ Sup	L	
Cluster4	Frontal _ Inf _ Tri	R	113
	Frontal_ Inf _ Oper	R	
	Frontal_ Mid	L	
Cluster5	Frontal _ Inf _ Tri	L	41
	Precentral	R	
Cluster6	Occipital _ Mid	R	28
Cluster7	Parietal _ Inf	L	215
	Occipital _ Mid	L	
	Angular	L	
Cluster8	Parietal _ Inf	R	96
	SupraMaginal	R	
Cluster9	Supp Motor Area	L	45
	Cingulum _ Mid	L	
Cluster10	Frontal_ Mid	L	61
	Frontal_ Sup	L	
	Precentral	L	
Cluster11	Frontal_ Sup	R	110
	Frontal_ Mid	R	

AAL: anatomical automatic labeling; L: left; R: right. Sup. = superior; Inf. = inferior; Mid. = middle.

subjected to paired-sample *t*-test. The results showed that the signals of the left inferior parietal, right triangle IFG, right superior frontal gyrus, right supramarginal gyrus, left middle frontal gyrus, left SMA, and the right orbital IFG were significantly higher during the TCO compared to the GNG paradigm (Fig. 5 A1 and A2).

Discussion

BIC is vital for human's adaptiveness, and is linked to several disorders, such as aggression, substance abuse, attention-deficit hyperactivity disorder, and schizophrenia (Smith et al., 2013; Bickel *et al.*, 2011; Alderson *et al.*, 2017; Cooper & Hughes, 2018). Although abundant research has investigated neural substrates of BIC during GNG task and stop signal task, these tasks were consistently shown to isolate neural processes of response inhibition, which is of primary interest, from those of response generation (Smith *et al.*, 2008). Accordingly, BIC-related neural substrates need to be re-examined using the TCO task, which is considered to be effective in controlling for these limitations (Yuan *et al.*, 2012; Zhao *et al.*, 2015). Therefore, using functional neuroimaging technique, the current study made a step forward for this purpose, with the design of a new task that allows for the comparison of the GNG and the TCO paradigm in outcome measures.

First of all, we observed that no-go and deviant conditions produced similar accuracy data, although both conditions exhibit a significantly reduced accuracy compared to the standard condition, as a result of the need for response inhibition and correspondent consumption of cognitive resources. This suggests that both the GNG and TCO task are effective in inducing the

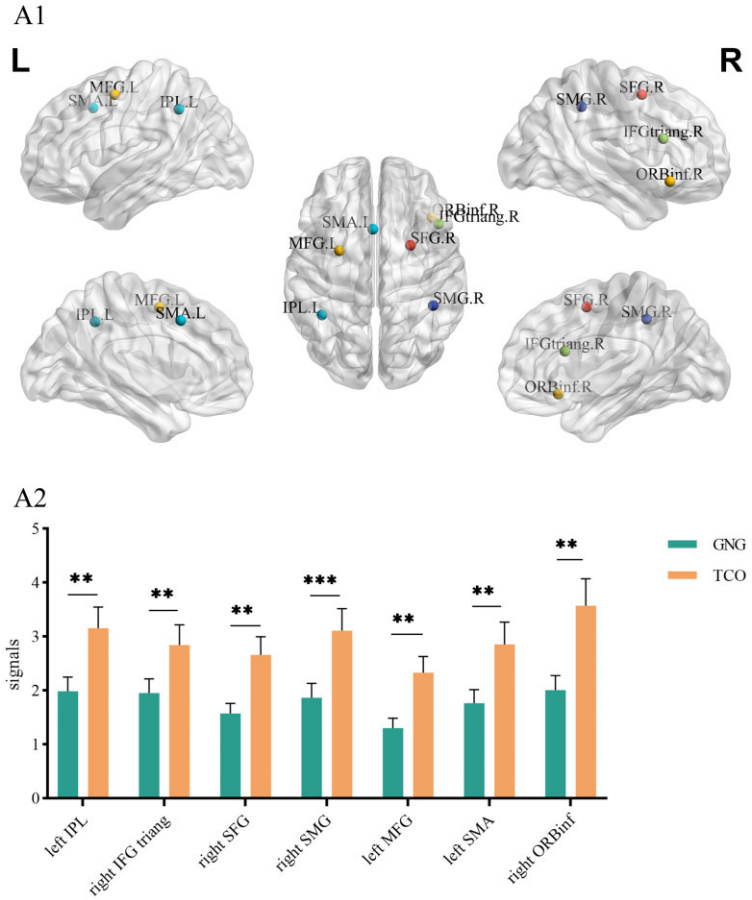

Figure 5: (A1) The regions where signals are significantly different in conjunction analysis during TCO and GNG conditions. (A2) Paired *t*-test of these regions in blood-oxygen-level-dependent signal (error bars denote SEM, $^{**}P < 0.01$; $^{***}P < 0.001$).

Table 4: Brain regions include cingulum cortex in TCO task and GNG task.

	Region (AAL)	Hemispheres	Voxel	*t*
TCO task (A1)	Supp _ Motor _ Area	L	47	8.00
		R	15	
	Cingulum _ Mid	L	29	
		R	15	
GNG task (A2)	Cingulum _ Ant	L	44	7.80
	Supp _ Motor _ Area	L	33	
	Frontal _ Sup _ Medial	L	32	
	Cingulum _ Mid	L	31	
		R	25	

AAL: anatomical automatic labeling; L: left; R: right. *t*-value denotes BIC effects over the survived regions for TCO and GNG task, respectively. Data are thresholded at FWE $P < 0.01$, with a cluster-level of $k > 20$

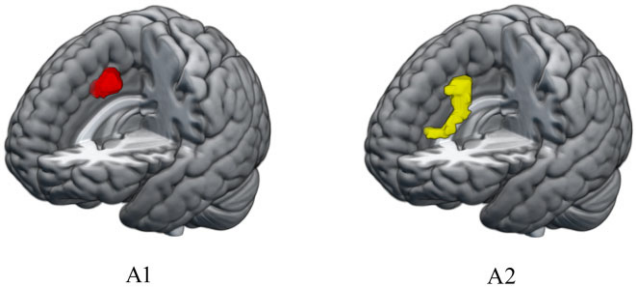

Figure 6: (A1): Middle cingulate cortex activation in TCO task. (A2): Anterior cingulate cortex activation in GNG task.

processes of BIC, to a similar extent. However, due to the design of dual responses, the TCO task provides an additional index of response time delay in deviant compared to standard condition, in that the accurate response to the deviant stimulus, which reengages a new motor response and entails an additional cognitive processing of inhibiting prepotent, habitual response to the standard stimulus. Thus, consistent with prior findings (Zhao *et al.*, 2015; Ren *et al.*, 2019), the results from the incorporated new paradigm used in the current study show that TCO task does provide more comprehensive behavioral indexes of BIC, as compared to the GNG or stop-signal task whose behavioral measure of BIC solely relies on the accuracy or stop-signal RT (Albert *et al.*, 2010; Li *et al.*, 2006).

In addition, the current fMRI results showed prominent activations of BIC-related cortical areas, consistent with the point that BIC is an integral process consisting of a series of collaborative elements (Yuan *et al.*, 2008; Li *et al.*, 2006). We found that the activation results for TCO and GNG were approximately the same, such as the shared activations in precuneus and IFG that are implicated in error detection/conflict monitoring, and inhibitory processing, respectively (Menon *et al.*, 2001; Aron *et al.*, 2014). Based on this, we used conjunction analysis to focus on the differences in the overlapping regions. The results indicate that the signals of TCO were significantly higher than those of GNG in the triangle and orbital areas of the inferior frontal cortex. The rIFG has been shown to send stop signals and inhibit automatic but irrelevant actions (Aron *et al.*, 2014; Sharp *et al.*, 2010; Chambers *et al.*, 2007). Combined with previous studies and our findings, we speculate that rIFG is an important node in the process of BIC, responsible for attention to task demand and the emission of inhibitory signals. Our current results not only validated the rIFG is task-independent and reaffirmed its important role in inhibitory control. Moreover, performing TCO compared to GNG task should involve more cognitive efforts indexed by the higher rIFG activations, probably as a result of dual motor responses rather than single response in GNG task.

Moreover, we found that ACC is not activated in TCO, whereas ACC activation is prominent in the GNG task (Fig. 6 and Table 4). ACC has been implicated to be responsible for the monitoring of erroneous responses and subsequent behavioral correction in previous BIC studies (Zhai *et al.*, 2019; Borst *et al.*, 2014; Fan, 2014; Wrege *et al.*, 2014; Bekker *et al.*, 2005). This suggests that the activation of the ACC is mainly caused by the monitoring of response conflicts. This account is also confirmed in interference resolution studies, such as those using the Stroop or Flanker interference tasks. In the process of interference resolution, participants are confronted with two simultaneous pieces of information, and they are required to respond to the relevant goal but suppress the irrelevant distractors (Zhang *et al.*, 2017). In TCO, the response to deviant stimuli is a combination of inhibitory control (inhibiting prepotent response) and motor re-engagement (generating alternative response). Thus, the design of dual motor responses in the TCO task may have mitigated the behavioral conflicts between motor inhibition and motor generation as evident in GNG task. This probably explains why we observed no significant activation of ACC during the performance of TCO.

Therefore, compared with GNG and SST that require participants to withhold or cancel motor action, the current findings show the uniqueness of TCO task in that it designs a component of re-engaging an alternative action in addition to the inhibition of a dominant response. In other words, when confronted with a deviant stimulus among a train of standard stimulus presentation, individuals do not perform withholding or cancellation of motor behavior, but instead choose an alternative behavior to replace the dominant motor response. This method has been thought to increase the ratio of successful inhibition, thereby may be useful in facilitating the rehabilitation of dominant, addictive behaviors (Zhao *et al.*, 2018). Therefore, future studies may adopt the TCO paradigm to explore the likelihood of improving the efficiency of addictive behavior intervention, probably through the current paradigm allowing the direct comparison of TCO and GNG. There are also limitations to be noted. The current study only compared the TCO with GNG paradigm in behavioral and neural measures of BIC, leaving the comparison of neural correlates between TCO and stop-signal task unanswered. Future studies also need to design a combined paradigm that realizes this comparison in a single study, to investigate the difference of neural substrates between them.

Supplementary Data

Supplementary data are available at *Psychoradiology Journal* online.

Author contributions

ZS-data analyses, presentation and paper writing. YR-study design, data collection and analysis, GW-data analysis and paper writing, LQ-data collection, YJ-conceptualization, study design, paper writing and supervision.

Conflict of Interest Statement

The authors declared no conflict of interests.

Acknowledgements

This study was supported by the national natural science foundation of China (NSFC31971018) and Sichuan distinguished young scholar fund (2023NSFSC1938).

References

Albert J, Lopez-Martin S, Carretie L (2010) Emotional context modulates response inhibition: neural and behavioral data. *Neuroimage* **49**:914–21.

Alderson RM, Patros CHG, Tarle SJ, *et al.* (2017) Working memory and behavioral inhibition in boys with ADHD: an experimental examination of competing models. *Child Neuropsychol* **23**:255–72.

Aron AR, Robbins TW, Poldrack RA (2004) Inhibition and the right inferior frontal cortex. *Trends Cogn Sci* **8**:170–7.

Aron AR, Robbins TW, Poldrack RA (2014) Inhibition and the right inferior frontal cortex: one decade on. *Trends Cogn Sci* **18**:177–85.

Behan B, Stone A, Garavan H (2015a) Right prefrontal and ventral striatum interactions underlying impulsive choice and impulsive responding. *Hum Brain Mapp* **36**:187–98.

Bekker EM, Kenemans JL, Verbaten MN (2005) Source analysis of the N2 in a cued go/no-go task. *Cognitive Brain Research* **22**:221–31.

Bellgrove MA, Chambers CD, Vance A, *et al.* (2006) Lateralized deficit of response inhibition in early-onset schizophrenia. *Psychol Med* **36**:495–505.

Bickel WK, Jarmolowicz DP, Mueller ET, *et al.* (2011) The behavioral economics and neuroeconomics of reinforcer pathologies: implications for etiology and treatment of addiction. *Curr Psychiatry Rep* **13**:406–15.

Bjork JM, Chen G, Hommer DW (2012) Psychopathic tendencies and mesolimbic recruitment by cues for instrumental and passively obtained rewards. *Biol Psychol* **89**:408–15.

Bokura H, Yamaguchi S, Kobayashi S (2001) Electrophysiological correlates for response inhibition in a go/no-go task. *Clinical Neurophysiol* **112**:2224–32

Borst G, Cachia A, Vidal J, *et al.* (2014) Folding of the anterior cingulate cortex partially explains inhibitory control during childhood: a longitudinal study. *Dev Cogn Neurosci* **9**:126–35.

Cai W, Leung HC (2009) Cortical activity during manual response inhibition guided by color and orientation cues. *Brain Res* **1261**:20–8.

Carter CS, Braver TS, Barch DM, *et al.* (1998) Anterior cingulate cortex, error detection, and the online monitoring of performance. *Science* **280**:747–9.

Chambers CD, Bellgrove MA, Gould IC, *et al.* (2007) Dissociable mechanisms of cognitive control in prefrontal and premotor cortex. *J Neurophysiol* **98**:3638–47.

Chao HH, Luo X, Chang JL, *et al.* (2009) Activation of the pre-supplementary motor area but not inferior prefrontal cortex in association with short stop signal reaction time—an intra-subject analysis. *BMC Neurosci* **10**:75.

Chao-Gan Y, Yu-Feng Z (2010) DPARSF: a MATLAB toolbox for "pipeline" data analysis of resting-State fMRI. *Front Systems Neurosci* **4**:13.

Chiu Y, Egner T (2015) Inhibition-induced forgetting. *Psychol Sci* **26**:27–38.

Cooper PS, Hughes ME (2018) Impaired theta and alpha oscillations underlying stopsignal response inhibition deficits in schizophrenia. *Schizophr Res* **193**:474–6.

Criaud M, Boulinguez P (2013) Have we been asking the right questions when assessing response inhibition in go/no-go tasks with fMRI? A meta-analysis and critical review. *Neurosci Biobehavl Rev* **37**:11–23.

Dong G, Lu Q, Zhou H, *et al.* (2010) Impulse inhibition in people with Internet addiction disorder: electrophysiological evidence from a go/No-go study. *Neurosci Lett* **485**:138–42.

Duann JR, Ide JS, Luo X, *et al.* (2009) Functional connectivity delineates distinct roles of the inferior frontal cortex and presupplementary motor area in stop signal inhibition. *J Neurosci* **29**:10171–9.

Duff EP, Cunnington R, Egan GF (2007) REX: response exploration for neuroimaging datasets. *Neuroinformatics* **5**:223–34.

Fan J (2014) An information theory account of cognitive control. *Front Human Neurosci* **8**:Article 680.

Friston KJ, Holmes AP, Price CJ, *et al.* (1999) Multisubject fMRI studies and conjunction analyses. *Neuroimage* **10**:385–96.

Garavan H, Ross TJ, Kaufman J, *et al.* (2003) A midline dissociation between error-processing and response-conflict monitoring. *Neuroimage* **20**:1132–9.

Goldstein M, Brendel G, Tuescher O, *et al.* (2007) Neural substrates of the interaction of emotional stimulus processing and motor inhibitory control: an emotional linguistic go/no-go fMRI study. *Neuroimage* **36**:1026–40.

Hester R, Fassbender C, Garavan H (2004) Individual differences in error processing: a review and reanalysis of three event-related fMRI studies using the go/no-go task. *Cerebral Cortex* **14**:986–94.

Houben K, Nederkoorn C, Wiers RW, *et al.* (2011) Resisting temptation: decreasing alcohol-related affect and drinking behavior by training response inhibition. *Drug Alcohol Depend* **116**:132–6.

Jahanshahi M, Obeso I, Rothwell JC, *et al.* (2015) A fronto–striato–subthalamic–pallidal network for goal-directed and habitual inhibition. *Nat Rev Neurosci* **16**:719–32.

Kok A, Ramautar JR, De Ruiter MB, *et al.* (2004) ERP components associated with successful and unsuccessful stopping in a stop-signal task. *Psychophysiology* **41**:9–20.

Korponay C, Dentico D, Kral TRA, *et al.* (2019) The effect of mindfulness meditation on impulsivity and its neurobiological correlates in healthy adults. *Sci Rep* **9**:11963.

Lee HW, Lu MS, Chen CY, *et al.* (2016) Roles of the pre-SMA and rIFG in conditional stopping revealed by transcranial magnetic stimulation. *Behav Brain Res* **296**:459–67.

Li CS, Huang C, Constable RT, *et al.* (2006) Imaging response inhibition in a stop-signal task: neural correlates independent of signal monitoring and post-response processing. *J Neurosci* **26**:186–92.

Logan GD, Cowan WB (1984) On the ability to inhibit thought and action: A theory of an act of control. *Psychol Rev* **91**:295–327.

Ma L, Steinberg JL, Cunningham KA, *et al.* (2015) Inhibitory behavioral control: a stochastic dynamic causal modeling study comparing cocaine dependent subjects and controls. *NeuroImage. Clin* **7**:837–47.

Mancini C, Falciati L, Maioli C, *et al.* (2022) Happy facial expressions impair inhibitory control with respect to fearful facial expressions but only when task-relevant. *Emotion* **22**:142–52.

Menon V, Adleman NE, White CD, *et al.* (2001) Error-related brain activation during a go/no-go response inhibition task. *Hum Brain Mapp* **12**:131–43.

Mostofsky SH, Simmonds DJ (2008) Response inhibition and response selection: two sides of the same coin. *J Cogn Neurosci* **20**:751–61.

Orr C, Hester R (2012) Error-related anterior cingulate cortex activity and the prediction of conscious error awareness. *Front Human Neurosci* **6**:177.

Qiu Z, Wang J (2021) Altered neural activities during response inhibition in adults with addiction: a voxel-wise meta-analysis. *Psychol Med* **51**:387–99.

Ren Z, Yang J, Yuan J (2019) Unconscious impulsivity control maintains the ability of behavioral inhibitory control in males: evidence of reaction-time cost. *Psych Journal* **8**:330–41.

Rubia K, Russell T, Overmeyer S, *et al.* (2001) Mapping motor inhibition: conjunctive brain activations across different versions of go/no-go and stop tasks. *Neuroimage* **13**:250–61.

Schel MA, Kühn S, Brass M, *et al.* (2014) Neural correlates of intentional and stimulus-driven inhibition: a comparison. *Front Human Neurosci* **8**:27.

Sharp DJ, Bonnelle V, De Boissezon X, *et al.* (2010) Distinct frontal systems for response inhibition, attentional capture, and error processing. *Proc Natl Acad Sci USA* **107**:6106–11.

Simmonds DJ, Pekar JJ, Mostofsky SH (2008) Meta-analysis of go/no-go tasks demonstrating that fMRI activation associated with response inhibition is task-dependent. *Neuropsychologia* **46**: 224–32.

Smith JL, Johnstone SJ, Barry RJ (2008) Movement-related potentials in the go/No-go task: the P3 reflects both cognitive and motor inhibition. *Clin Neurophysiol* **119**:704–14.

Smits DJM, Boeck PD, Vansteelandt K (2004) The inhibition of verbally aggressive behaviour. *Eur J Pers* **18**:537–55.

Suárez-Suárez S, Doallo S, Pérez-García JM, *et al.* (2020) Response inhibition and binge drinking during transition to university: an fMRI study. *Front Psychiatry* **11**:535.

Todd RM, Lewis MD, Meusel L, *et al.* (2008) The time course of social-emotional processing in early childhood: ERP responses to facial affect and personal familiarity in a go-No-go task. *Neuropsychologia* **46**:595–613.

Wang Y, Braver TS, Yin S, *et al.* (2019) Reward improves response inhibition by enhancing attentional capture. *Soc Cogn Affect Neurosci* **14**:35–45.

Wilbertz T, Deserno L, Horstmann A, *et al.* (2014) Response inhibition and its relation to multidimensional impulsivity. *Neuroimage* **103**:241–8.

Wolpe N, Hezemans FH, Rae CL, *et al.* (2022) The pre-supplementary motor area achieves inhibitory control by modulating response thresholds. *Cortex* **152**:98–108.

Wöstmann NM, Aichert DS, Costa A, *et al.* (2013) Reliability and plasticity of response inhibition and interference control. *Brain Cogn* **81**:82–94.

Wrege J, Schmidt A, Walter A, *et al.* (2014) Effects of cannabis on impulsivity: a systematic review of neuroimaging findings. *Curr Pharm Des* **20**:2126–37.

Yu F, Yuan J, Luo Y (2009) Auditory-induced emotion modulates processes of response inhibition: an event-related potential study. *Neuroreport* **20**:25–30.

Yuan J, He Y, Qinglin Z, *et al.* (2008) Gender differences in behavioral inhibitory control: ERP evidence from a two-choice oddball task. *Psychophysiology* **45**:986–93.

Yuan J, Liu W, Liang Q, *et al.* (2020) Effect of low-frequency repetitive transcranial magnetic stimulation on impulse inhibition in abstinent patients with methamphetamine addiction. *JAMA Network Open* **3**:e200910.

Yuan J, Meng X, Yang J, *et al.* (2012) The valence strength of unpleasant emotion modulates brain processing of behavioral inhibitory control: neural correlates. *Biol Psychol* **89**:240–51.

Yuan J, Xu M, Yang J, *et al.* (2017) The application of the two-choice oddball paradigm to the research of behavioral inhibitory control (in Chinese). *Sci Sin Vitae* **47**:1065–73

Zavala B, Zaghloul K, Brown P (2014) The subthalamic nucleus, oscillations, and conflict. *Mov Disord* **30**:328–38.

Zhai ZW, Yip SW, Lacadie CM, *et al.* (2019) Childhood trauma moderates inhibitory control and anterior cingulate cortex activation during stress. *Neuroimage* **185**:111–8.

Zhang R, Geng X, Lee TMC (2017) Large-scale functional neural network correlates of response inhibition: an fMRI meta-analysis. *Brain Struct Funct* **222**:3973–90.

Zhao X, Liu X, Maes JHR (2018) Male smokers' behavioral and brain responses to deviant cigarette-related stimuli in a two-choice oddball paradigm. *J Psychophysiol* **32**:172–81.

Zhao X, Ting L, Yi Z, *et al.* (2015) Response inhibition of cigarette-related cues in male light smokers: behavioral evidence using a two-choice oddball paradigm. *Front Psychol* **6**:1506.

Received: 25 May 2023; **Revised:** 21 June 2023; **Accepted:** 20 July 2023